



Cite this: *Green Chem.*, 2016, **18**, 6586

Isobutylene-rich imidazolium ionomers for use in two-phase partitioning bioreactors†

Stuart L. Bacon, Andrew J. Daugulis* and J. Scott Parent*

Imidazolium ionomer derivatives of an isobutylene-rich elastomer demonstrated superior absorption characteristics for target molecules of biological interest compared to their non-ionic parent material, while retaining biocompatibility with a range of suspended cell cultures. Halide displacement from brominated poly(isobutylene-co-paramethyl styrene) was used to introduce 0.23 mmol per g-polymer of imidazolium bromide functionality to the polymer, resulting in up to 10-fold improvements in *n*-octanol and *n*-butanol partition coefficients (PCs) and up to 4-fold improvements in selectivity (α). In contrast to analogous imidazolium ionic liquids (ILs) that were cytotoxic toward *Saccharomyces cerevisiae*, *Clostridium acetobutylicum* and *Pseudomonas putida*, the ionomers had no effect on suspended cell growth. In addition, these ionomers demonstrated surface antimicrobial activity towards select microorganisms under static conditions with direct surface/microbe contact. Thus, these materials do not affect suspended cell growth while simultaneously reducing cell proliferation at the ionomer interface.

Received 12th August 2016,
Accepted 7th October 2016

DOI: 10.1039/c6gc02251k

www.rsc.org/greenchem

1. Introduction

Bioprocesses that are hindered by substrate and/or product cytotoxicity can be improved using two-phase partitioning bioreactor (TPPB) technology, which mitigates cell inhibition by sequestering toxic target molecule(s) into an immiscible second phase. TPPB configurations can be applied to the biodegradation of xenobiotics, where the polymer phase serves as a reservoir for delivering a cytotoxic substrate at sub-lethal concentrations, as well as extractive fermentation, where the polymer is used to remove a cytotoxic product from the fermentation medium as it is formed. For bioremediation applications TPPBs have been effectively exploited for the treatment of contaminated gas,¹ aqueous,² and soil³ environments, as has been recently reviewed.⁴ In biosynthesis applications, a recent review article has described TPPB advances over the past decade,⁵ and another recent review⁶ has evaluated the factors that are important in selecting an effective TPPB sequestering phase. Effective TPPB absorbents provide high solute affinity, as quantified by the partition coefficient (PC), and a strong preference for solute absorption *versus* water uptake, as quantified by selectivity ($\alpha_{i/w} = PC_{\text{solute}}/PC_{\text{water}}$). The latter is particularly important for extractive fermentation processes (notably for bio-fuels), whose cost effectiveness and energy requirements can be sensitive to the efficiency of solute recovery processes.

Absorbent selection and design must also include biocompatibility assessments to ensure that biocatalyst growth and metabolism is not adversely affected by the sequestering phase.

Viscoelastic polymers have emerged as promising TPPB materials, demonstrating favourable absorption characteristics, facile separation from the fermentation medium, and biocompatibility towards suspended cell cultures.^{7–10} Furthermore, their solid-state physical properties offer operational advantages over low MW organic solvents and oligomeric liquids, which can present foaming, emulsification and volatility problems.^{11–14} However, shifting focus from small molecule absorbing phases to polymeric absorbents requires consideration of crystallinity and glass transition temperature (T_g), since neither crystalline domains nor glassy phases are capable of solute uptake.^{15,16} TPPB processes involving non-polar solutes (*e.g.* PAHs, BTEX, styrene) are relatively straightforward, since these target molecules are readily absorbed by non-polar polymers that have low T_g and little affinity for water. In contrast, hydrophilic solutes such as *n*-butanol require more polar polymers that can be glassy at bioprocessing temperatures, thereby limiting solute removal to surface adsorption.

Separation processes based on ionic liquids (IL)^{17–20} have benefited greatly from the ability to adjust solute affinities by varying both cation and anion structure.^{21–26} As such, their use in TPPBs has gained recent interest, however, their utility is often limited by microbe cytotoxicity.^{27–31} We have found that isobutylene-rich elastomers bearing small amounts of covalently-bound IL functionality (ionomers) provide the absorption characteristics, physical properties and biocompatibility needed to support a broad spectrum of TPPB applications.

Department of Chemical Engineering, Queen's University, 19 Division St., Kingston, Ontario, Canada K7L 3N6. E-mail: daugulis@queensu.ca, parent@queensu.ca

†Electronic supplementary information (ESI) available. See DOI: 10.1039/c6gc02251k

These ionomers are easy to prepare *via* nucleophilic displacement of halide from brominated poly(isobutylene-*co*-paramethylstyrene) (BIMS)³² to yield amorphous, rubbery derivatives comprised of a non-polar isobutylene-rich polymer matrix and aggregated ion-pairs known as multiplets.³³

This report provides complex viscosity (η^*), PC, $\alpha_{i/w}$, biocompatibility, and surface antimicrobial data for BIMS-based

ionomers with a range of cation (butylimidazolium, hydroxyethylimidazolium) and anion (Br^- , BF_4^-) structures (Table 1). Oscillatory rheology measurements of η^* are used to demonstrate differences in the physical properties of viscoelastic ionomers and viscous ILs. This is followed by comprehensive PC and α data for three solutes relevant to TPPBs (*n*-butanol, *n*-octanol and styrene) that explore differences in absorption

Table 1 Room temperature properties of ionomer and IL absorbents

Sample ID	Structure	Ion pair concentration (mmol per g)	Physical state	Complex viscosity η^* (Poise)	Equilibrium water absorption (wt%)
BIMS		0	Viscoelastic solid	342 000	3.5 ± 1.8
IMS-[HEIm][Br]		0.23	Viscoelastic solid	1 236 000	11.5 ± 2.2
IMS-[BuIm][Br]		0.23	Viscoelastic solid	807 000	13.3 ± 2.8
IMS-[BuIm][BF ₄]		0.23	Viscoelastic solid	642 000	9.2 ± 0.6
[C ₁₂ BuIm][Br]		2.68	Viscous liquid	37.3	Water soluble
[C ₁₂ BuIm][BF ₄]		2.63	Viscous liquid	10.6	6.3 ± 0.3

for solutes of different hydrophobicity and types of molecular interaction. Absorbent biocompatibility in a well-mixed TPPB environment is assessed for industrially-relevant microorganisms (*Saccharomyces cerevisiae*, *Pseudomonas putida*, *Clostridium acetobutylicum*) before quantifying surface antimicrobial characteristics by measuring microorganism colony proliferation under prolonged, direct contact with the polymer. This material property is linked to biofilm formation and surface fouling and is pertinent to any material that is in sustained contact with microorganisms.^{34–36}

2. Experimental

2.1 Materials

Butyl imidazole (98%), 1-bromododecane (97%), trifluoroethanol (99%), sodium tetrafluoroborate (NaBF₄) (98%), sodium sulfate (Na₂SO₄) (98%), styrene (99%) and *n*-octanol (99%) were purchased from Sigma-Aldrich (Canada). Methanol (99.8%) and *n*-butanol (99%) were purchased from Fischer Scientific (Canada). All chemicals were used as received. Brominated poly(isobutylene-*co*-paramethylstyrene) (BIMS) (EXXPRO 3745, 0.23 mmol benzylic bromide functionality per g BIMS) ($M_n > 50\,000\text{ g mol}^{-1}$) was supplied by Exxon Mobil Chemical (Baytown, Texas) and purified prior to use by dissolving in THF and precipitating in excess acetone, followed by drying *in vacuo* at RT.

2.2 Synthesis of IMS-[BuIm][Br] and IMS-[HEIm][Br]

BIMS (40 g, 9.2 mmol benzylic bromide) was dissolved in toluene (400 mL). Butyl imidazole (2.287 g, 2 eq.) or hydroxyethyl imidazole (2.063 g, 2 eq.) was added to the polymer cement and heated to 100 °C under nitrogen for 7 h (IMS-[BuIm][Br]) or 16 h (IMS-[HEIm][Br]). Conversion was measured by ¹H-NMR integration of residual brominated paramethylstyrene mers: δ 4.49 (s, 2H), δ 4.45 (s, 2H). The product was recovered from precipitation in excess acetone, milled into thin sheets and dried *in vacuo* at 60 °C. **IMS-[BuIm][Br]:** ¹H-NMR (CDCl₃ + 5 wt% CD₃OD): δ 9.99 (s, 1H, -N⁺-CH-N-), δ 5.43 (s, 2H, Ph-CH₂-N⁺-), δ 4.27 (t, 2H, -N-CH₂-CH₂-CH₂-CH₃). **IMS-[HEIm][Br]:** ¹H-NMR (CDCl₃ + 5 wt% CD₃OD): δ 9.55 (s, 1H, -N⁺-CH-N-), δ 5.36 (s, 2H, Ph-CH₂-N⁺-), δ 4.39 (t, 2H, -N-CH₂-CH₂-OH).

2.3 Synthesis of IMS-[BuIm][BF₄]

IMS-[BuIm][Br] (40 g, 9.2 mmol bromide) was dissolved in toluene (600 mL). NaBF₄ (4.00 g, 36.8 mmol, 4 eq.) was dissolved in ultrapure water (100 mL) and added to the polymer cement. The mixture, which formed an emulsion upon agitation, was stirred for 8 h and then left to settle overnight forming an aqueous phase, a polymer rich phase and a toluene rich phase. The aqueous phase was removed by pipette, then fresh NaBF₄ brine was added (4.00 g NaBF₄ in 100 mL) and again stirred to emulsion for 8 hours. Removal and replenishment of the brine was repeated twice over until ion exchange was complete within experimental error. The

emulsion was precipitated in excess acetone, milled into thin sheets and dried *in vacuo* at 60 °C. **¹H-NMR** (CDCl₃ + 5 wt% CD₃OD): δ 9.03 (s, 1H, -N⁺-CH-N-), δ 5.31 (s, 2H, Ph-CH₂-N⁺-), δ 4.19 (t, 2H, -N-CH₂-CH₂-CH₂-CH₃). **¹⁹F-NMR** (CDCl₃ + 5 wt% CD₃OD): δ -152.75 (s, 4F, ¹¹BF₄), δ -152.79 (s, 4F, ¹⁰BF₄). Ion exchange conversion was measured by ¹⁹F-NMR integration of tetrafluoroborate peaks using a trifluoroethanol internal standard. Note that ¹⁰BF₄ and ¹¹BF₄ are isotopomers that exist in a 4 : 1 ratio.

2.4 Synthesis of [C₁₂BuIm][Br]

Butyl imidazole (10 g, 80.5 mmol) and 1-bromododecane (24.9 g, 100 mmol, 1.25 eq.) were dissolved in ethyl acetate (25 mL) and stirred for 24 h at reflux under nitrogen. The solution was dried *in vacuo* at 50 °C to yield the product, 1-dodecyl-3-butylimidazolium bromide ([C₁₂BuIm][Br]), as an orange oil. The product was washed several times with hexanes to remove residual 1-bromododecane, dried *in vacuo* at 50 °C and characterized by ¹H-NMR. Yield: 87%. **¹H-NMR** ((CD₃)₂SO): δ -9.25 (s, 1H, -N⁺-CH-N-), δ -7.82 (d, 2H, -N-CH=CH-N⁺-), δ -4.17 (m, 4H, -N-CH₂-CH₂-), δ -1.78 (m, 4H, -N-CH₂-CH₂-), δ -1.23 (m, 20H, -(CH₂)₁₁-CH₃), δ -0.90 (t, 3H, -(CH₂)₃-CH₃), δ -0.85 (t, 3H, -(CH₂)₁₁-CH₃).

2.5 Synthesis of [C₁₂BuIm][BF₄]

NaBF₄ (7.6 g, 69.6 mmol, 1.0 eq.) was slowly added to a solution of [C₁₂BuIm][Br] (26 g, 69.6 mmol) dissolved in ultrapure water (500 ml) at 70 °C under nitrogen. The mixture was stirred for 24 h, with an additional 1.0 eq. of NaBF₄ (7.6 g) added after 3 h. The ion exchange yielded the product 1-dodecyl-3-butylimidazolium tetrafluoroborate ([C₁₂BuIm][BF₄]) as a yellow oil. The oil was dissolved in toluene (50 mL), separated and washed twice with NaBF₄ brine (15.2 g, 2 eq. in 50 mL). Residual water in the toluene phase was removed using Na₂SO₄ and then dried *in vacuo* at 50 °C. The product was characterized by ¹H-NMR and ¹⁹F-NMR using trifluoroethanol as an internal standard. Yield: 88%. **¹H-NMR** ((CD₃)₂SO): δ -9.18 (s, 1H, -N⁺-CH-N-), δ -7.80 (d, 2H, -N-CH-CH-N⁺-), δ -4.16 (m, 4H, N-CH₂-CH₂-), δ -1.78 (m, 4H, -N-CH₂-CH₂-), δ -1.24 (m, 20H, -(CH₂)₁₀-CH₃), δ -0.90 (t, 3H, -(CH₂)₃-CH₃), δ -0.86 (t, 3H, -(CH₂)₁₁-CH₃). **¹⁹F-NMR** ((CD₃)₂SO): δ -149.26 (s, 4F, ¹¹BF₄), δ -149.31 (s, 4F, ¹⁰BF₄), δ -76.23 (t, 3F, CF₃CH₂OH).

2.6 Partition coefficient (PC) experiments

Solute PC tests were performed in triplicate as previously described¹⁶ using aqueous solutions of styrene (0.2 g L⁻¹), octanol (0.4 g L⁻¹) and butanol (10 g L⁻¹) in Type I ultrapure water. For styrene and octanol PC tests, the absorbent phase fraction was 1 wt%. For butanol PCs, the absorbent fraction was 5 wt%. In addition to the polymer mass, a 10 mL aliquot of styrene, octanol or butanol aqueous solution were added to each scintillation vial, sealed tightly with a foil lined cap and allowed to equilibrate in an Innova 4400 incubator shaker at 30 °C at 180 rpm for 1 week. Aqueous solute concentrations before and after equilibration with the polymer were measured using a Varian

450-GC gas chromatography unit equipped with a CP-8410 AutoInjector, VF-5 ms 30 m capillary column and FID detector.

A TA Instruments Q500 thermogravimetric analyzer to determine total water/solute uptake. Polymer/IL samples (10–15 mg) soaked in styrene, octanol or butanol solutions were pat dry and immediately heated in a TA Instruments Q500 thermogravimetric analyzer from ~25 °C to 200 °C (20 °C min⁻¹). The samples were held at 200 °C (styrene bp 145 °C; octanol bp 195 °C; butanol bp 118 °C) until the rate of mass loss dropped below 0.05 wt% min⁻¹.

A mass balance was performed to determine the solute concentration in the polymer phase. Experimental PC values were calculated using aqueous and polymer phase weight fractions (w_i^{aq} and w_i^{poly}) of the solute and water in eqn (1). Standard deviation values were calculated from triplicate samples to establish a mean value for the equilibrium PC.

$$PC_i = \frac{w_i^{\text{poly}}}{w_i^{\text{aq}}} \quad (1)$$

Solute/water selectivity ($\alpha_{i/w}$) was calculated as in eqn (2).

$$\alpha_{i/w} = \frac{PC_i}{PC_w} \quad (2)$$

2.7 Microorganisms and media

Saccharomyces cerevisiae was obtained from Alltech (Nicholasville, Kentucky) and cultivated in a medium from Doran and Bailey³⁷ containing 10 g L⁻¹ glucose, 5 g L⁻¹ KH₂PO₄, 2 g L⁻¹ yeast extract, 2 g L⁻¹ (NH₄)₂SO₄, 0.4 g L⁻¹ MgSO₄·7H₂O, and 0.1 g L⁻¹ CaCl₂. *Pseudomonas putida* ATCC 11172 was cultured in the 'LM medium' described by Fujita *et al.*³⁸ containing 10 g L⁻¹ glucose, 10 g L⁻¹ bacto-peptone, 5 g L⁻¹ Bacto-yeast, and 5 g L⁻¹ NaCl. *Clostridium acetobutylicum* ATCC 824 was cultured anaerobically in 'Medium A' described by Barton & Daugulis,³⁹ modified to 10 g L⁻¹ glucose. *p*-Aminobenzoic acid and biotin were prepared separately in a 1000× solution and sterilized through a 0.45 μm filter.

2.8 Biocompatibility testing

Growth media were freshly prepared and 50 mL added to 125 mL Erlenmeyer flasks using a burette. Foam plugs were added to the flasks, loosely covered with aluminum foil, then the flasks were autoclaved. Once cool, 5 g of sterile IL or polymer (cut into 2 mm cubes) was aseptically added to the flasks. To *C. acetobutylicum* cultures, 0.05 mL of sterile *p*-aminobenzoic acid and biotin solution was also added at this point. The *C. acetobutylicum* cultures were then sealed with a sterile fold-over rubber stopper and sparged aseptically for 5 min, alternating between oxygen-free N₂ gas and vacuum every 30 seconds to ensure anaerobic conditions.

Cultures were inoculated with 2 mL of -80 °C glycerol stock culture and incubated at 180 rpm and 30 °C (*S. cerevisiae* and *P. putida*) or 37 °C (*C. acetobutylicum*). After 24 h, cell growth was determined through triplicate optical density measurements at 600 nm (OD₆₀₀) using a Biochrom Ultraspec 3000 UV/

Visible Spectrophotometer, with Type I ultrapure water as a reference. Polymer and IL biocompatibility was determined by comparing OD₆₀₀ to duplicate control cultures.

2.9 Antimicrobial surface behaviour

Antimicrobial testing was performed as previously described,^{40,41} with minor microbe and polymer-specific modifications. In this work, polymer samples were dissolved (5 wt%) in toluene (BIMS) or 98 : 2 toluene : hexanol solution (ionomer), cast (1.5 mL) onto glass microscope slides (75 × 25 mm) and allowed to dry *in vacuo* for 48 h. An overnight culture of *S. cerevisiae*, *P. putida* or *C. acetobutylicum* was used to inoculate (10% v/v) 50 mL of fresh media and incubated at 30 °C or 37 °C and 180 rpm for 4–6 hours. After centrifugation (3500 rpm, 5 min; IEC 3000R centrifuge), the cells were re-suspended in Type I ultrapure water to an OD₆₀₀ ~0.10 (*S. cerevisiae*) or 0.001 (*P. putida*, *C. acetobutylicum*). The microbial suspension was sprayed onto the test surfaces using a commercial chromatography sprayer (VWR scientific) using sterile nitrogen gas (10 psi). After drying (3–4 min), the glass slide was placed in a petri dish and molten agar (1.5 wt% agar, autoclaved, cooled to 40 °C) was carefully added. The petri dish was sealed and incubated at 30 °C overnight. To facilitate anaerobic growth of *C. acetobutylicum*, molten agar was sparged with N₂ during cooling and petri dish samples were incubated, unsealed at 37 °C under a sterile N₂ environment. Microbial colonies were counted after 24 h using a colony counter. Experiments were performed in duplicate.

2.10 Complex viscosity (η^*)

Polymers were tested at 30 °C using an Advanced Polymer Analyzer 2000 (Alpha Technologies) controlled-strain rheometer equipped with biconical discs operating at 1 Hz and 0.5° arc. Ionic liquids were tested at 25 °C using an Anton Paar MCR 702 rheometer equipped with parallel plates operating in the linear viscoelastic region at 1 Hz and 0.1–10% shear strain.

3. Results and discussion

3.1 Physical properties of ionomers and ILs

Efficient TPPB operation requires that the two phases are easily separated, with the aqueous fermentation medium recycled immediately, and the non-aqueous phase processed for solute removal/regeneration before being returned to the bioprocess. As described above, polymeric absorbents are well suited to this application, owing to their solid-like characteristics. Consider the complex viscosity (η^*) data listed in Table 1, which quantify the dynamic response of a material to an applied oscillatory strain. Unlike the steady-shear viscosity measurements used routinely for low molecular weight (MW) liquids, dynamic measurements can be applied to viscous liquids (*e.g.* ILs) as well as high MW polymers.¹⁰ The tabulated data (Table 1) show that BIMS and its ionic derivatives provide η^* values 4 to 5-orders of magnitude greater than the ILs, clearly establishing them as viscoelastic solids as opposed to viscous liquids.

The small amount of functionality within our ionomers (0.23 mmol per g-polymer) is insufficient to affect the glass transition temperature, which remains unchanged from the BIMS value of approximately $T_g = -22$ °C.⁴² As such, these materials are amorphous, rubbery polymers at bioprocessing temperatures. As a result, these materials are capable of absorbing solute throughout their bulk. It should be noted, however, that the morphology of ionomers is more complex than for non-ionic polymers, in that poor solvation of bound ion-pairs results in aggregation of ionic functionality. Evidence of ion-pair association is found in our η^* measurements of BIMS and its imidazolium ionomer derivatives. Depending on ion-pair structure, η^* values increased 1.9–3.6-fold over the parent material (Table 1), owing to polymer chain mobility restrictions imposed by the ionic network.⁴³ These η^* gains approach those generated by covalent crosslinking formulations, yet these ionomers remain completely soluble in suitable organic solvents. The impact of imidazolium-based multi-plets on solute uptake is detailed below.

3.2 Solute absorption

Biodegradation and biosynthesis are well-established 'green' processes, with the TPPB technology platform offering process intensification benefits that are proportional to absorptive performance (PC and α). TPPB target solutes can span the entire range from hydrophobic (e.g. PAHs, BTEX, styrene) to hydrophilic (e.g. organic acids, alcohols). We selected three solutes – styrene, 1-octanol, and 1-butanol – to examine the influence of ionic functionality on the absorption of different solute classes. These molecules are also relevant to bioprocessing, in that styrene is a xenobiotic that is amenable to TPPB technology,^{44,45} octanol is a widely used reference for assessing compound hydrophobicity ($\log K_{o/w}$),⁴⁶ and butanol's development as a renewable biofuel, suffers from strong product inhibition.

Solute properties that are often used to interpret thermodynamic equilibrium data are listed in Table 2. $\log K_{o/w}$ values identify butanol as the most hydrophilic compound of the three, while differences between octanol and styrene are not resolved by this measure. Hansen solubility parameters (HSP) are more informative, as they quantify dispersive (δ_D), hydrogen-bonding (δ_H) and polar (δ_P) interactions for pure materials, thereby differentiating styrene from the two alcohols. HSP values for ionomers and ionic liquids are not available. However, data for poly(isobutylene) (PIB), whose composition

is very similar to that of BIMS, allow for the calculation of the Hansen Ra distance (eqn (3)) from the target solutes to the non-ionic parent material. The smaller the Ra value, the greater the thermodynamic affinity of the polymer for a solute. On this basis, PC data for BIMS acting on the target solutes is expected to follow the order; styrene > octanol > butanol.

$$Ra = \sqrt{4*(\delta_{D,1} - 16.9)^2 + (\delta_{P,1} - 2.5)^2 + (\delta_{H,1} - 4.0)^2}. \quad (3)$$

These predictions are borne out by experiment, with BIMS providing a styrene PC of 180 ± 6 (Fig. 1a). Furthermore, the hydrophobic character of the BIMS polymer backbone is reflected by an $\alpha_{s/w}$ value of 6200 ± 250 (Fig. 1b), demonstrating a strong preference for styrene over water. Note that both PC and α for a polymer-solute-water system are not constants, but depend on solute activities in the aqueous and organic phases and, by extension, are functions of mixture composition.⁵⁰ The data reported throughout this work were acquired using a standard experimental condition to facilitate comparisons between polymers.

Chemical modification of BIMS to introduce an ion-pair concentration of 0.23 mmol per g-polymer improved styrene uptake at the expense of selectivity, with only minor differences recorded for the various ionomer compositions, as shown in Fig. 1a and d. These data show that ionic functionality that is capable of ion-dipole and hydrogen bonding interactions prefers associating with water over a non-polar solute. In the context of TPPB technology, heightened water uptake is not problematic, since styrene biodegradation is less concerned with absorption selectivity than total absorption capacity.

Although octanol and styrene have similar $\log K_{o/w}$ values ($\log K_{o/w} = [\text{Solute}]_{\text{octanol}}/[\text{Solute}]_{\text{aqueous}}$; Table 2), they differ markedly in terms of their absorption by BIMS, with an octanol PC of just 11 ± 3 (Fig. 1b) and an $\alpha_{o/w}$ value of 360 ± 90 (Fig. 1e). This is consistent with the estimated HSP Ra of 7.8 for the BIMS-octanol system. Of greater interest is the effect of imidazolium bromide functionality on octanol absorption, which increased the octanol PC 9.2–10-fold and its $\alpha_{o/w}$ value 3–3.7-fold. The latter improvement is particularly important, since it demonstrates the potential for imidazolium bromide functionality to increase alcohol absorption selectively over water absorption. Exchange of the Br^- counter ion with BF_4^- compromised both PC_{OctOH} and $\alpha_{o/w}$, confirming that absorption affinity and selectivity for polar solutes can move in parallel.

The butanol absorption data were consistent with that recorded for octanol, with the imidazolium bromide derivative providing PC_{BuOH} values about 10 times that of BIMS (Fig. 1c), and selectivity about 4-fold greater (Fig. 1f). The importance of this result to TPPB process efficiency and intensification cannot be overstated. *Clostridium sp.*, a widely used biocatalyst for butanol production, suffers product inhibition at titres of $12\text{--}16$ g L⁻¹, thereby establishing an upper aqueous concentration limit for a TPPB fermentation process.^{51,52} Higher PC values mean that less polymer is needed to keep butanol levels

Table 2 Thermodynamic properties of BIMS and solutes of interest

	$\log K_{o/w}$	δ_D	δ_P	δ_H	Hansen Ra from PIB
Styrene ^{a,b}	2.95	18.6	1.0	4.1	3.7
1-Octanol ^{a,b}	3.00	16.0	5.0	11.2	7.8
1-Butanol ^{a,b}	0.88	16.0	5.6	15.8	12.3
Poly(isobutylene) ^b	—	16.9	2.5	4.0	—

^a $\log K_{o/w}$ data sourced from ref. 47. ^b HSP data sourced from ref. 48 and 49.

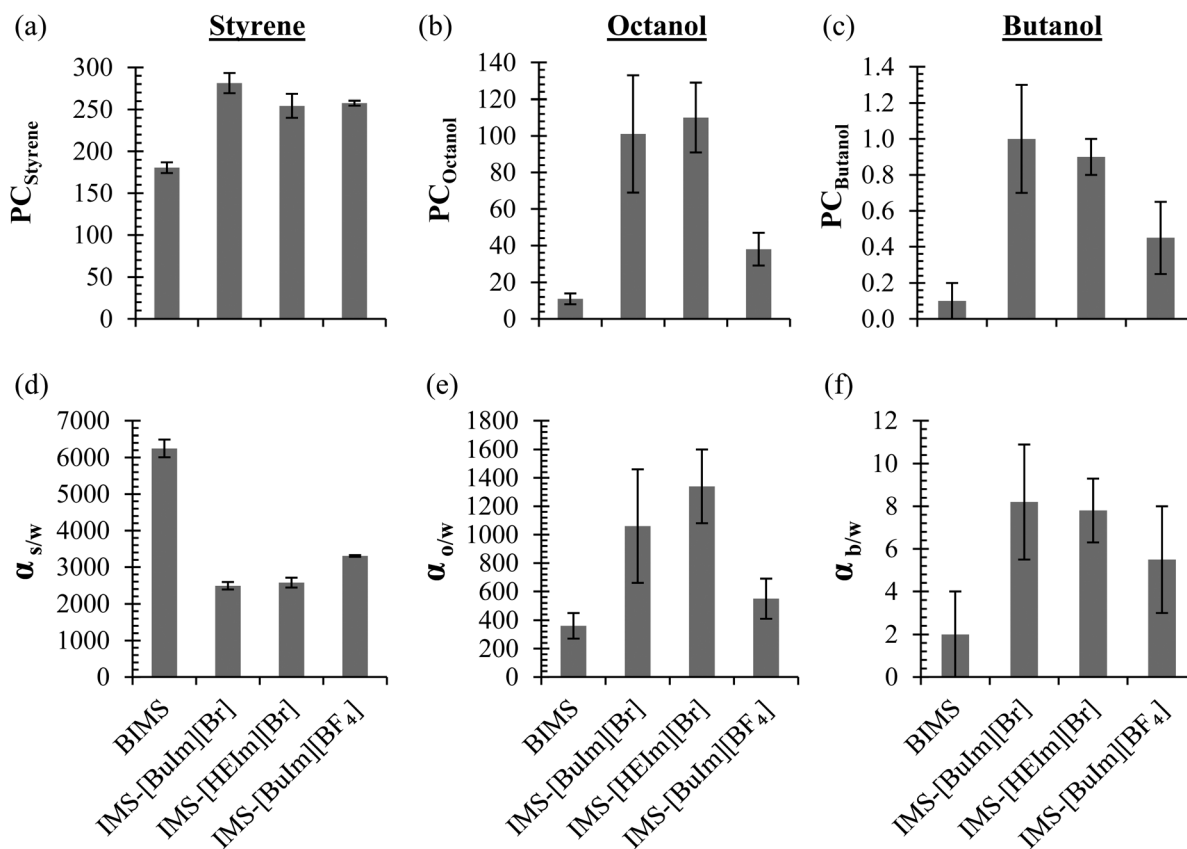


Fig. 1 Partition coefficient (PC) (a, b, c) and solute/water selectivity (α) (d, e, f) for styrene, octanol and butanol in BIMS and its ionic derivatives (0.23 mmol-ion pair per g-polymer).

below this target, resulting in better volumetric productivity in the bioreactor. Superior selectivity values concentrate butanol in the polymer phase at the expense of water, thereby improving the energy efficiency of butanol purification by a subsequent separation process.⁵³

3.3 Comparison of solute absorption in ionomers and ionic liquids

Insight into absorptive differences between the ionomers of present interest and IL systems was gained by examining two materials, $[C_{12}BuIm][Br]$ and $[C_{12}BuIm][BF_4]$. Both are viscous liquids at bioprocessing temperatures (Table 1), but the bromide salt is miscible with water and, hence, inappropriate as a TPPB absorbent. Interestingly, $IMS-[BuIm][Br]$ was

amongst the best performing ionomers developed in this work (Fig. 1). By rendering the ion-pair insoluble with water, covalent binding to an isobutylene-rich backbone made it useful for solute absorption. This suggests that ionomer development efforts can target hydrophilic IL functionality in an effort to promote selective alcohol uptake.

The more hydrophobic tetrafluoroborate salt, $[C_{12}BuIm][BF_4]$, formed an IL phase when mixed with water, and proved highly absorbent toward all three solutes (Table 3). Indeed, it generated the highest PC and selectivity results recorded in this study. The butanol extraction data are in the range of previous reports on related ILs, $[C_6Mim][BF_4]$ and $[C_8Mim][BF_4]$, which produced similar PC (0.9 and 2.2) and selectivity (3.9 and 12.2) values.⁵⁴ Taken together, these results

Table 3 Comparison of PC and water/solute selectivity between BIMS, ionomer and IL absorbents

Absorbent	Ion pair conc. (mmol g ⁻¹)	Styrene		Octanol		Butanol	
		PC _{Styrene}	$\alpha_{s/w}$	PC _{OctOH}	$\alpha_{o/w}$	PC _{BuOH}	$\alpha_{b/w}$
BIMS	0	181 ± 6	6200 ± 250	11 ± 3	360 ± 90	0.1 ± 0.1	2 ± 2
IMS-[BuIm][BF ₄]	0.23	257 ± 3	3300 ± 30	38 ± 9	550 ± 140	0.4 ± 0.2	5 ± 2
IMS-[BuIm][Br]	0.23	281 ± 12	2500 ± 100	101 ± 32	1060 ± 400	1.0 ± 0.3	8 ± 3
[C ₁₂ BuIm][BF ₄]	2.63	343 ± 57	6700 ± 1000	311 ± 17	11 200 ± 1100	3.3 ± 0.2	101 ± 9
[C ₁₂ BuIm][Br]	2.68	n/a – soluble		n/a – soluble		n/a – soluble	

demonstrate the superior absorptive properties of pure ILs relative to ionomer analogues. However, their utility as TPPB absorbents is predicated on their biocompatibility, which is explored below.

3.4 Biocompatibility

As defined by IUPAC,⁵⁵ biocompatibility refers to the “ability of a material to be in contact with a biological system without producing an adverse effect.” In the context of TPPB development, biocompatibility is judged by a material’s effect on suspended cell cultures in a well-mixed aqueous medium,⁵⁶ typically using a 10 wt% second phase fraction.^{57,58} Several indicators of biological activity, including cell growth and glucose consumption, have been exploited successfully for these assessments.⁵⁷ In this work we evaluated ILs and ionomers by measuring cell growth *via* the optical density (600 nm) of *S. cerevisiae*, *P. putida* and *C. acetobutylicum* in a TPPB environment. These microorganisms are well-represented in literature,^{59–61} with *S. cerevisiae* an industrial ethanol-producing yeast (eukaryote) and a pertinent delivery vehicle for genetic engineering, *P. putida* a Gram-negative bacterium widely used in bioremediation applications, and *C. acetobutylicum* a common butanol-producing Gram-positive bacterium.

The two ILs ([C₁₂BuIm][Br] and [C₁₂BuIm][BF₄]) were not biocompatible, severely hindering microbial growth relative to a single phase control (Fig. 2). These results align with previous reports of [BuMIm][BF₄] toxicity (~1% (v/v)) towards the yeast *Pichia pastoris* and the bacteria *Escherichia coli* and *Bacillus cereus*.⁶² More generally, reports of IL cytotoxicity towards a broad spectrum of microorganisms, mammalian cell lines and aquatic organisms^{28,30,63–65} suggest that some

ILs present biocompatibility concerns when used in two-phase bioprocesses. Consequently, while two-phase bioprocesses are generally considered to be ‘green’, the use of ILs in these cases introduces toxicity precluding their use.

In contrast, covalently grafting the imidazolium functionality in our ionomers substantially eliminated cytotoxicity, as evidenced by the optical density data recorded for all three ionomers, across all cell types. The grafting approach is distinct from previous heterogeneous polymer/IL blends,^{66–69} in which a dispersed IL phase is not polymer-bound and can leach into the cell-containing aqueous phase. Altogether, we have demonstrated that IL cytotoxicity can be mitigated by covalently grafting the IL to an insoluble polymer backbone. This approach facilitates the use of a broader selection of ion-pair functionality, particularly those with promising thermodynamic properties that are limited by their water solubility and cytotoxicity in IL form.

3.5 Antimicrobial surface properties

The control of microbial growth on surfaces has critical process implications on the operation of TPPBs and related membrane separations (*e.g.* pervaporation, ultrafiltration, reverse osmosis),^{36,70} since biofilm formation can provide a diffusional barrier and compromise the rate of solute transport into the polymer.^{71–75} Therefore, antimicrobial surfaces that kill microbes and/or prevent their colonization at the interface have attracted considerable attention.^{34,36,76,77} These materials include polymers equipped with imidazolium,^{78,79} pyridinium,⁴⁰ phosphonium⁸⁰ and ammonium functionality,³⁴ each demonstrating varying degrees of surface antimicrobial activity.

The biocompatibility experiments described above showed that our ionomers had no significant effect on suspended microbe growth that takes place in the bulk aqueous medium (OD₆₀₀). We have extended these studies by investigating microbe/ionomer interactions directly at the material interface. This involved a standard antimicrobial surface testing procedure first developed by Tiller *et al.*⁴⁰ and applied successfully elsewhere.^{41,81,82} Briefly, a cell suspension was sprayed evenly onto a polymer surface, allowed to dry, and then covered with nutrient-rich agar to ensure direct microbe/polymer contact. After incubation, microbial colonies were counted relative a non-ionic BIMS control slide.

The ionomer surfaces demonstrated the strongest antimicrobial activity toward the yeast *S. cerevisiae*, reducing colony formation between 95–98.5% compared to BIMS (Fig. 3). Interestingly, they were not as potent towards bacteria, with total *P. putida* colonies reduced by 51–64% and no significant change in *C. acetobutylicum* colony proliferation. Reports suggest that antimicrobial activity stems from an ability to disrupt the microorganism’s cell wall and/or phospholipid membrane.^{40,41,83} Thus, structural differences between microbes may explain the observed microbe-dependent potency. For example, the thicker and more robust peptidoglycan layer of the Gram-positive *C. acetobutylicum* bacterium may enable greater resistance to membrane disruption. In

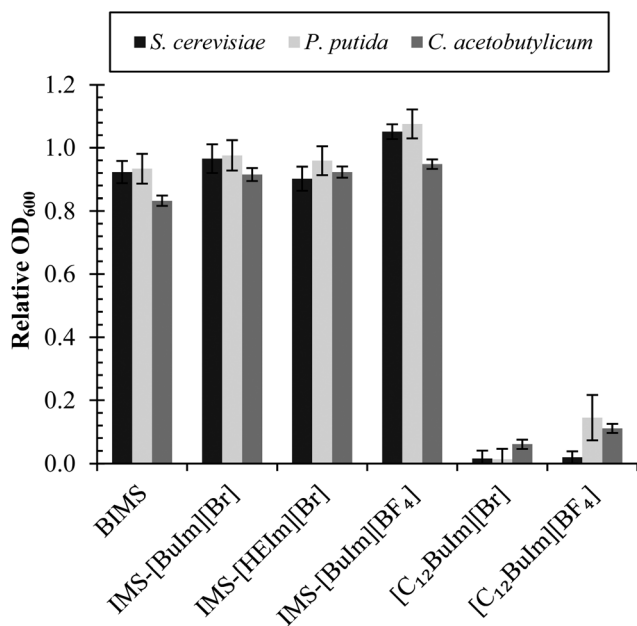


Fig. 2 Optical density (24 h) of suspended cell cultures in contact with 10% (wt/v) BIMS, ionomer or IL.

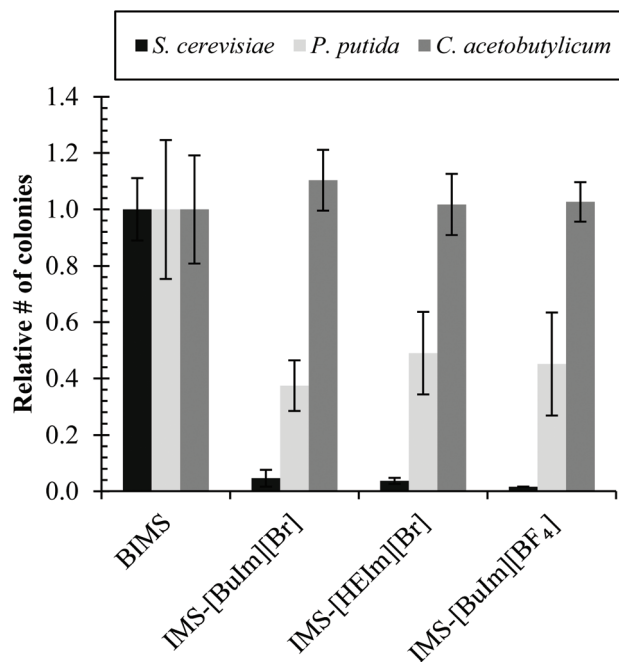


Fig. 3 Antimicrobial activity of the ionomers relative to BIMS (representative images can be found in ESI†).

addition to differences in cell structure, material surface charge density can also have an impact on antimicrobial activity. Previous reports suggest that there exists a bacterium-specific threshold below which antimicrobial activity is significantly reduced.^{81,84} Given the low levels of ionic functionality (0.23 mmol per g-polymer) in our materials, this may account for the observed microbe-dependent potency.

In all, these results demonstrate that a material can be biocompatible towards suspended cell culture while simultaneously possessing surface antimicrobial behaviour under static conditions. The combination of biocompatibility and antimicrobial properties is ideal for TPPB and membrane-based product recovery techniques, enabling bulk cell growth while minimizing cell proliferation and biofilm formation at the interface.

4. Conclusions

Introducing 0.23 mmol per g-polymer of imidazolium-based ionic functionality to an isobutylene-rich elastomer produced ionomers with a broader range of solute absorption characteristics. Partition coefficients for styrene, octanol and butanol were enhanced, but selectivity improvements were limited to alcohol absorption. Whereas imidazolium-based ILs were not biocompatible with suspended cultures of *S. cerevisiae*, *P. putida* and *C. acetobutylicum*, their respective ionomers were suitable for TPPB applications. Furthermore, the ionomers provide surface antimicrobial activity towards some microorganisms under prolonged, direct contact.

Abbreviations

BIMS	Brominated poly(isobutylene-co-paramethylstyrene)
IMS-[BuIm][Br]	<i>n</i> -Butylimidazolium bromide derivative of BIMS
IMS-[HEIm][Br]	2-Hydroxyethylimidazolium bromide derivative of BIMS
IMS-[BuIm][BF ₄]	<i>n</i> -Butylimidazolium tetrafluoroborate derivative of BIMS
[C ₁₂ BuIm][Br]	1-Dodecyl-3-butylimidazolium bromide
[C ₁₂ BuIm][BF ₄]	1-Dodecyl-3-butylimidazolium tetrafluoroborate

Acknowledgements

We gratefully acknowledge the financial support of DuPont Canada and the Natural Sciences and Engineering Research Council of Canada.

References

- C. T. Davidson and A. J. Daugulis, *Appl. Microbiol. Biotechnol.*, 2003, **62**, 297–301.
- G. P. Prpich, L. Rehmann and A. J. Daugulis, *Biotechnol. Prog.*, 2008, **24**, 839–844.
- L. Rehmann, G. P. Prpich and A. J. Daugulis, *Chemosphere*, 2008, **73**, 798–804.
- R. Muñoz, A. J. Daugulis, M. Hernández and G. Quijano, *Biotechnol. Adv.*, 2012, **30**, 1707–1720.
- W. Van Hecke, G. Kaur and H. De Wever, *Biotechnol. Adv.*, 2014, **32**, 1245–1255.
- J. T. Dafoe and A. J. Daugulis, *Biotechnol. Lett.*, 2014, **36**, 443–460.
- M. C. Tomei, M. C. Annesini, S. Rita and A. J. Daugulis, *Environ. Sci. Technol.*, 2010, **44**, 7254–7259.
- D. R. Nielsen and K. J. Prather, *Biotechnol. Bioeng.*, 2009, **102**, 811–821.
- M. Montes, A. J. Daugulis, M. C. Veiga and C. Kennes, *J. Chem. Technol. Biotechnol.*, 2011, **86**, 47–53.
- S. L. Bacon, A. J. Daugulis and J. S. Parent, *Chem. Eng. J.*, 2016, **299**, 56–62.
- G. Quijano, M. Hernandez, F. Thalasso, R. Muñoz and S. Villaverde, *Appl. Microbiol. Biotechnol.*, 2009, **84**, 829–846.
- A. Arca-Ramos, G. Eibes, M. T. Moreira, G. Feijoo and J. M. Lema, *Chem. Eng. J.*, 2014, **240**, 281–289.
- L. D. Collins and A. J. Daugulis, *Biotechnol. Bioeng.*, 1997, **55**, 155–162.
- J. L. Rols, J. S. Condoret, C. Fonade and G. Goma, *Biotechnol. Bioeng.*, 1990, **35**, 427–435.
- S. L. Bacon, J. S. Parent and A. J. Daugulis, *J. Chem. Technol. Biotechnol.*, 2014, **89**, 948–956.
- S. L. Bacon, E. C. Peterson, A. J. Daugulis and J. S. Parent, *Biotechnol. Prog.*, 2015, **31**, 1500–1507.

- 17 M. Zawadzki, F. A. E. Silva, U. Domańska, J. A. P. Coutinho and S. P. M. Ventura, *Green Chem.*, 2016, **18**, 3527–3536.
- 18 R. J. Cornmell, C. L. Winder, S. Schuler, R. Goodacre and G. Stephens, *Green Chem.*, 2008, **10**, 685–691.
- 19 U. Domańska and M. Królikowski, *J. Chem. Thermodyn.*, 2012, **53**, 108–113.
- 20 K. S. Khachatryan, S. V. Smirnova, I. I. Torocheshnikova, N. V. Shvedene, A. A. Formanovsky and I. V. Pletnev, *Anal. Bioanal. Chem.*, 2005, **381**, 464–470.
- 21 W. Y. Lou, M. H. Zong and T. J. Smith, *Green Chem.*, 2006, **8**, 147–155.
- 22 A. B. Pereiro, J. M. M. Araujo, J. M. S. S. Esperanca, I. M. Marrucho and L. P. N. Rebelo, *J. Chem. Thermodyn.*, 2012, **46**, 2–28.
- 23 L. D. Simoni, A. Chapeaux, J. F. Brennecke and M. A. Stadtherr, *Comput. Chem. Eng.*, 2010, **34**, 1406–1412.
- 24 H. Zhao, S. Xia and P. Ma, *J. Chem. Technol. Biotechnol.*, 2005, **80**, 1089–1096.
- 25 P. Steltenpohl and E. Gracsová, *Acta Chim. Slovaca*, 2014, **7**, 129–133.
- 26 P. Dehury, U. Mahanta and T. Banerjee, *Fluid Phase Equilib.*, 2016, DOI: 10.1016/j.fluid.2016.06.007.
- 27 R. Melgarejo-Torres, C. O. Castillo-Araiza, P. López-Ordaz, N. V. Calleja-Castañeda, J. L. Cano-Velasco, R. M. Camacho-Ruiz, G. J. Lye and S. Huerta-Ochoa, *Chem. Eng. J.*, 2015, **279**, 379–386.
- 28 O. Dipeolu, E. Green and G. Stephens, *Green Chem.*, 2009, **11**, 397.
- 29 M. Matsumoto, K. Mochiduki, K. Fukunishi and K. Kondo, *Sep. Purif. Technol.*, 2004, **40**, 97–101.
- 30 A. Romero, A. Santos, J. Tojo and A. Rodríguez, *J. Hazard. Mater.*, 2008, **151**, 268–273.
- 31 K. M. Docherty and C. F. Kulpa, Jr., *Green Chem.*, 2005, **7**, 185.
- 32 J. S. Parent, A. M. J. Porter, M. R. Kleczek and R. A. Whitney, *Polymer*, 2011, **52**, 5410–5418.
- 33 E. B. Anderson and T. E. Long, *Polymer*, 2010, **51**, 2447–2454.
- 34 Y. Liu, C. Leng, B. Chisholm, S. Stafslie, P. Majumdar and Z. Chen, *Langmuir*, 2013, **29**, 2897–2905.
- 35 A. Kugel, S. Stafslie and B. J. Chisholm, *Prog. Org. Coat.*, 2011, **72**, 222–252.
- 36 I. Francolini, G. Donelli, F. Crisante, V. Taresco and A. Piozzi, in *Biofilm-based healthcare-associated infections: Volume II (Advances in Experimental Medicine and Biology)*, ed. G. Donelli, 2015, vol. 831, pp. 93–117.
- 37 P. M. Doran and J. E. Bailey, *Biotechnol. Bioeng.*, 1986, **28**, 73–87.
- 38 M. Fujita, M. Ike and T. Kamiya, *Water Res.*, 1993, **27**, 9–13.
- 39 W. E. Barton and A. J. Daugulis, *Appl. Microbiol. Biotechnol.*, 1992, **36**, 632–639.
- 40 J. C. Tiller, C. J. Liao, K. Lewis and A. M. Klibanov, *Proc. Natl. Acad. Sci. U. S. A.*, 2001, **98**, 5981–5985.
- 41 S. Krishnan, R. J. Ward, A. Hexemer, K. E. Sohn, K. L. Lee, E. R. Angert, D. A. Fischer, E. J. Kramer and C. K. Ober, *Langmuir*, 2006, **22**, 11255–11266.
- 42 A. R. Cillero, *Synthesis and reinforcement of peroxide-cured butyl rubber thermosets*, Queen's University, 2014.
- 43 J. S. Parent, A. Liskova, R. A. Whitney and R. Resendes, *J. Polym. Sci., Part A: Polym. Chem.*, 2005, **43**, 5671–5679.
- 44 S. M. Zamir, S. Babatabar and S. A. Shojaosadati, *Chem. Eng. J.*, 2015, **268**, 21–27.
- 45 P. Parnian, S. M. Zamir and S. A. Shojaosadati, *Chem. Eng. J.*, 2016, **284**, 926–933.
- 46 OECD, *OECD Guideline for the Testing of Chemicals - Partition Coefficient (n-octanol/water): Shake Flask Method*, Paris, 1995.
- 47 C. Hansch, A. Leo and D. Hoekman, *Exploring QSAR: Volume 2: Hydrophobic, Electronic, and Steric Constants*, ACS Publications, Washington, 1st edn, 1995.
- 48 C. M. Hansen, *Hansen Solubility Parameters: A User's Handbook*, Taylor & Francis Group, Boca Raton, FL, 2nd edn, 2007.
- 49 S. Abbott and H. Yamamoto, HSPiP Computer Program v. 5.0.04, 2013.
- 50 S. L. Bacon, J. Scott Parent and A. J. Daugulis, *J. Chem. Technol. Biotechnol.*, 2014, **89**, 948–956.
- 51 D. T. Jones and D. R. Woods, *Microbiol. Rev.*, 1986, **50**, 484–524.
- 52 F. Monot, J. R. Martin, H. Petitdemange and R. Gay, *Appl. Environ. Microbiol.*, 1982, **44**, 1318–1324.
- 53 M. Matsumura, H. Kataoka, M. Sueki and K. Araki, *Bioprocess*, 1988, **3**, 93–100.
- 54 S. H. Ha, N. L. Mai and Y.-M. Koo, *Process Biochem.*, 2010, **45**, 1899–1903.
- 55 M. Vert, Y. Doi, K.-H. Hellwich, M. Hess, P. Hodge, P. Kubisa, M. Rinaudo and F. Schué, *Pure Appl. Chem.*, 2012, **84**, 1.
- 56 R. Muñoz, S. Arriaga, S. Hernández, B. Guieysse and S. Revah, *Process Biochem.*, 2006, **41**, 1614–1619.
- 57 L. D. Collins and A. J. Daugulis, *Appl. Microbiol. Biotechnol.*, 1999, **52**, 354–359.
- 58 R. Muñoz, M. Chambaud, S. Bordel and S. Villaverde, *Appl. Microbiol. Biotechnol.*, 2008, **79**, 33–41.
- 59 S. Ostergaard, L. Olsson and J. Nielsen, *Microbiol. Mol. Biol. Rev.*, 2000, **64**, 34–50.
- 60 S. Y. Lee, J. H. Park, S. H. Jang, L. K. Nielsen, J. Kim and K. S. Jung, *Biotechnol. Bioeng.*, 2008, **101**, 209–228.
- 61 I. Pobleto-Castro, J. Becker, K. Dohnt, V. M. Dos Santos and C. Wittmann, *Appl. Microbiol. Biotechnol.*, 2012, **93**, 2279–2290.
- 62 F. Ganske and U. T. Bornscheuer, *Biotechnol. Lett.*, 2006, **28**, 465–469.
- 63 M. Matsumoto, K. Mochiduki and K. Kondo, *J. Biosci. Bioeng.*, 2004, **98**, 344–347.
- 64 H. R. Cascon, S. K. Choudhari, G. M. Nisola, E. L. Vivas, D. J. Lee and W. J. Chung, *Sep. Purif. Technol.*, 2011, **78**, 164–174.
- 65 G. Quijano, A. Couvert and A. Amrane, *Bioresour. Technol.*, 2010, **101**, 8923–8930.
- 66 S. Heitmann, J. Krings, P. Kreis, A. Lennert, W. R. Pitner, A. Górak and M. M. Schulte, *Sep. Purif. Technol.*, 2012, **97**, 108–114.

- 67 Y. T. Ong, K. F. Yee, Y. K. Cheng and S. H. Tan, *Sep. Purif. Rev.*, 2014, **43**, 62–88.
- 68 S. Livi, V. Bugatti, B. G. Soares and J. Duchet-Rumeau, *Green Chem.*, 2014, **16**, 3758.
- 69 A. Hasanoğlu, *Desalin. Water Treat.*, 2015, **3994**, 1–13.
- 70 C. G. Kumar and S. Anand, *Int. J. Food Microbiol.*, 1998, **42**, 9–27.
- 71 S. F. Zhang, A. Splendiani, L. M. Freitas dos Santos and A. G. Livingston, *Biotechnol. Bioeng.*, 1998, **59**, 80–89.
- 72 Z. Dong, G. Liu, S. Liu, Z. Liu and W. Jin, *J. Membr. Sci.*, 2014, **450**, 38–47.
- 73 S. Nakao, F. Saitoh, T. Asakura, T. Kiyoshi and S. Kimura, *J. Membr. Sci.*, 1987, **30**, 273–287.
- 74 A. Garcia III, E. L. Iannotti and J. L. Fischer, *Biotechnol. Bioeng.*, 1986, **28**, 785–791.
- 75 M. Cheryan, *Ultrafiltration Handbook*, Technomic Publishing Co., Inc., Lancaster, PA, 1987.
- 76 E. R. Kenawy, S. D. Worley and R. Broughton, *Biomacromolecules*, 2007, **8**, 1359–1384.
- 77 F. Siedenbiedel and J. C. Tiller, *Polymer*, 2012, **4**, 46–71.
- 78 B. Izmaylov, D. Di Gioia, G. Markova, I. Aloisio, M. Colonna and V. Vasnev, *React. Funct. Polym.*, 2015, **87**, 22–28.
- 79 M. Colonna, C. Berti, E. Binassi, M. Fiorini, S. Sullalti, F. Acquasanta, M. Vannini, D. Di Gioia, I. Aloisio, S. Karanam and D. J. Brunelle, *React. Funct. Polym.*, 2012, **72**, 133–141.
- 80 A. Kanazawa, T. Ikeda and T. Endo, *Antimicrob. Agents Chemother.*, 1994, **38**, 945–952.
- 81 J. C. Tiller, S. B. Lee, K. Lewis and A. M. Klibanov, *Biotechnol. Bioeng.*, 2002, **79**, 465–471.
- 82 D. Park, J. A. Finlay, R. J. Ward, C. J. Weinman, S. Krishnan, M. Paik, K. E. Sohn, M. E. Callow, J. A. Callow, D. L. Handlin, C. L. Willis, D. A. Fischer, E. R. Angert, E. J. Kramer and C. K. Ober, *ACS Appl. Mater. Interfaces*, 2010, **2**, 703–711.
- 83 L. Timofeeva and N. Kleshcheva, *Appl. Microbiol. Biotechnol.*, 2011, **89**, 475–492.
- 84 R. Kügler, O. Bouloussa and F. Rondelez, *Microbiology*, 2005, **151**, 1341–1348.